Nanoscale Advances

ROYAL SOCIETY OF CHEMISTRY

MINIREVIEW

View Article Online
View Journal | View Issue

Cite this: *Nanoscale Adv.*, 2020, **2**, 3624

A perspective on oxide-supported single-atom catalysts

Junyi Zhou, Zhen Xu, Meijia Xu, Xiong Zhou* and Kai Wu *

Single-atom catalysts (SACs) can not only maximize the metal atom utilization efficiency, but also show drastically improved catalytic performance for various important catalytic processes. Insights into the working principles of SACs provide rational guidance to design and prepare advanced catalysts. Many factors have been claimed to affect the performance of SACs, which makes it very challenging to clarify the correlation between the catalytic performance and physicochemical characteristics of SACs. Oxide-supported SACs are one of the most extensively explored systems. In this minireview, some latest developments on the determining factors of the stability, activity and selectivity of SACs on oxide supports are overviewed. Discussed also are the reaction mechanisms for different systems and methods that are employed to correlate the properties with the catalyst structures at the atomic level. In particular, a recently proposed surface free energy approach is introduced to fabricate well-defined modelled SACs that may help address some key issues in the development of SACs in the future.

Received 15th May 2020
Accepted 14th July 2020

DOI: 10.1039/d0na00393j

rsc.li/nanoscale-advances

1 Introduction

In recent years, single-atom catalysts (SACs) or alternatively single site catalysts (SSCs) with isolated metal atoms dispersed on solid supports have drawn tremendous attention and accordingly very rapid progress has been achieved.[1–6] People have been fascinated by the unique properties that SACs have exhibited in specific reactions, including minimum loading of precious metal atoms to reach maximum catalytic efficiency. The concept of the 'SAC' was initially proposed by Zhang and co-workers in their pioneering work in 2011.[7] They successfully synthesized a SAC that consists of isolated Pt atoms anchored to the surface of iron oxide. Ever since, a dramatically increased number of SACs with a promising catalytic performance have been designed and fabricated, together with careful structural characterization for the dispersion of the metallic species. However, it's also well known that aimlessly and endlessly downsizing the metal particles does not necessarily guarantee a better catalytic performance.[8–15] The so-called "size effect" is too simplified to explain various phenomena that have been experimentally observed in different catalytic reactions by all sorts of SACs. In addition, not only does the single atom matter in reactions, but the environment including the oxide support and the metal–support interaction also plays a critical role in the catalytic performance. Historically, the "ensemble effect" has long been proposed and applied in designing novel heterogeneous catalysts because many supported metal catalysts require specific reaction sites that are formed by either metal atoms or metal–support contacts. Thus, it is meaningful to find concrete intrinsic principles to elucidate this ensemble effect. Despite the rapid progress and valuable insights, the intrinsic principles of SACs still remain elusive, which in return spurs further explorations in SACs.

In terms of the configuration of the single atoms supported on oxides, there exist some general considerations without subtle inspections of specific SAC cases and their structural details.[16–24] In general, the surface free energy of a bulk metal increases significantly as its size decreases. To obtain thermally stable single metal atoms on oxides, one approach is to strengthen the metal–oxide interaction so that the metal atoms could highly disperse rather than aggregate into clusters. Meanwhile, ultrathin oxide films may serve as a new group of structural support materials whose surface free energy and adhesion to the added metals can be fine-tuned by the film thickness, providing another approach to stabilize the single atoms. Therefore, adoption of either a strong metal interaction or an ultrathin oxide film becomes the pre-requisite for the development of these SACs.

Furthermore, the oxide support may act as an oxygen reservoir that stores and releases oxygen, and takes part in redox reactions *via* a Mars–van Krevelen (MvK) mechanism.[25] The absence of neighbouring metal atoms in SACs obviously generates a maximum metal–oxide contact, leading to a fascinating metal–support interface effect that promotes redox reactions. The charge state of a metal particle essentially remains close to neutrality because the transferred electrons at the interface are shared by abundant atoms in the particle, while the partially transferred charge is localized at the single atoms, resulting in a crucial charge effect on the performance of

BNLMS, College of Chemistry and Molecular Engineering, Peking University, Beijing 100871, China. E-mail: kaiwu@pku.edu.cn; xiongzhou@pku.edu.cn

SACs. Low coordination is often regarded as a common characteristic of SACs, though it is not necessary that single atoms may be highly coordinated to the oxide support, and attributed to be responsible for their high activity. Moreover, owing to their limited number of available metal sites, SACs are conceived to have limitations for complex reactions, which can be alternatively applied to improve the selectivity of SACs under certain circumstances.

Quite a few reviews on SACs have been published in the past decades and provided excellent overviews of this rapidly growing research field.[26–43] These reviews have already summarized synthetic strategies, structural characterization, and/or catalytic evaluations for specific reactions. In this minireview, we instead try to provide a fundamental understanding of the intrinsic principles of SACs in their catalytic performance with some very recent typical case studies in the past years. Given that stability, activity and selectivity are three main assessment indexes for catalytic performance, the following section will be framed in this sequence, aiming at illuminating the connotations that make SACs unique and different from supported metal nanoparticles. In addition, we also provide our perspective on the surface free energy approach recently developed by our group and our understanding of reaction mechanisms on oxide-supported SACs.

2 Stability improvement

One of the key issues in the development of SACs is how to stabilize the single metal atoms under practical reaction conditions. In common situations, metal atoms on oxides are too facile to diffuse and aggregate into nanoparticles to lower their surface free energy or chemical potential, which spontaneously triggers the Ostwald ripening process at elevated temperatures. Many efforts have been devoted to retaining the atomic dispersion state of the unstable metal atoms. Herein, we summarize some main aspects to describe the development of the stability of SACs.

2.1 Metal–oxide interaction

Conventionally, SACs are routinely prepared by wet chemistry which includes impregnation, co-precipitation and deposition–precipitation. In this way, metal atoms may be stabilized by the strong metal–oxide interaction *via* either their incorporation into solid lattices or replacement of metal cations in oxides. Physical deposition is another powerful methodology to prepare highly dispersed SACs under high-vacuum conditions for fundamental research. Regardless of preparation methods, the anchoring position of single atoms in/on oxides can be divided into three types: type a, location on the oxide surfaces; type b, replacement of the surface metal cations; and type c, incorporation into the oxide lattices.

Interestingly, Jakub *et al.* have reported a study of the $Ir_1/Fe_3O_4(001)$ (where Ir_1 stands for a single Ir atom) model catalyst that contains all three types of SACs mentioned above and provided a direct estimation of their stability.[44] As shown in Fig. 1, Ir single atoms are obtained by deposition onto the

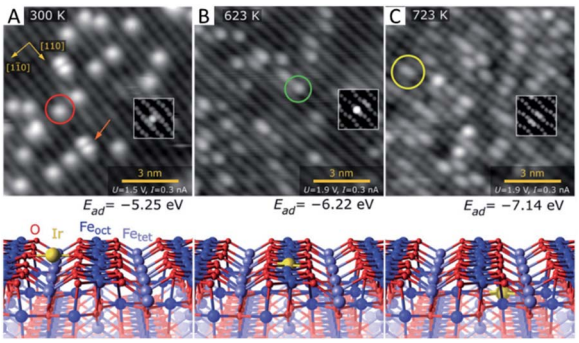

Fig. 1 Local structure of $Ir_1/Fe_3O_4(001)$ determined by room-temperature STM (up) and the corresponding DFT model (down). (A) 2-fold coordinated Ir_1 atom on $Fe_3O_4(001)$ prepared at 300 K. (B) 5-fold coordinated Ir atom incorporated within the $Fe_3O_4(001)$ surface after thermal annealing at 623 K. (C) 6-fold coordinated Ir adatom incorporated into the subsurface layer of $Fe_3O_4(001)$ after thermal annealing at 723 K. Reproduced with permission.[44] Copyright 2019, Wiley-VCH.

$Fe_3O_4(001)$ surface at 300 K (Fig. 1A). The Ir single atoms are experimentally observed to be located in between two neighbouring lattice oxygens with a 2-fold coordination. The adsorption energy per Ir atom is 5.25 eV according to DFT calculations. These Ir single atoms are unstable and can be transformed into a 5-fold coordination geometry upon thermal treatment at 623 K (Fig. 1B). They displace the surface iron cations with an increase in their adsorption energy up to 6.22 eV. When the model catalyst is further warmed up to 723 K (Fig. 1C), the Ir atoms are incorporated into the subsurface layer to become 6-fold coordinated. The adsorption energy further increases to 7.14 eV, and the Ir single atoms eventually aggregate into metallic Ir clusters as the sample temperature is elevated to 900 K.

Obviously, highly coordinated single atoms incorporated into the subsurface (type c) have the highest stability. In such a situation, the catalytic performance is, however, largely affected because the active metal atoms are no longer in direct contact with the reactants. It is therefore necessary to retain the atomic dispersion state of the active and unstable metal atoms in order to balance their high catalytic activity. Great efforts have been made to create plenty of real cases where the balance can be indeed achieved and the existence of the metal–oxide interaction is confirmed as well.

Meier *et al.*[45] have proven that the $Fe_3O_4(001)$ surface can stabilize ordered arrays of metal adatoms (Ag and Cu) with a high thermal stability up to 550 K. The metal adatoms do occupy the bulk-continuation cation sites above the surface and become two-fold coordinated to the surface oxygen atoms (type a). Zhang *et al.*[46] have reported a highly stable and atomically dispersed Pt catalyst supported on mesoporous Al_2O_3 that survives CO oxidation between 100 °C and 400 °C for one month. The Pt atoms are firmly anchored to the inner surface of the support, occupying the unsaturated pentahedral Al^{3+} centres and coordinating with four oxygen anions (type b). Kim *et al.*[87] have successfully synthesized Pt SACs on antimony-doped tin oxide (Pt_1/ATO) by incipient wet impregnation and

demonstrated that the single Pt atoms survive repeated cyclic voltammetry for 1800 cycles where the Pt_1/ATO serves as the anode catalyst. The stability stems from the replacement of the Sb atoms with Pt in the ATO support (type b).

2.2 Protecting functional groups or gaseous adsorbents

Except the oxide itself, other extrinsic functional groups or gaseous adsorbates have been introduced to stabilize SACs. Thang *et al.*[47] have explored the nature of the stability of single Pt atoms on anatase TiO_2. The Pt atoms bind to two excess oxygen atoms on the surface (PtO_2), which arise from the formation of surface hydroxyl groups and provide a solid anchor to the oxide support. They also suggest that the stability of atomically dispersed Ru atoms on ZrO_2 originates from the interaction of the Ru atoms with one OH group of the surface with elimination of H_2 by condensation, leaving the RuO species strongly bound to the zirconia surface.[48] Millet *et al.*[49] have prepared Ni SACs on MgO *via* co-precipitation. The catalysts stay stable between 200 °C and 300 °C over 100 h on stream without sintering. The stability relates to the formation of hydrogenated carbonate species on the surface during the reactions.

Interestingly, Duan *et al.*[50] have synthesized a series of high Pt_1 density Pt_1/Fe_2O_3 SACs (Fig. 2A) by a facile wet chemical method and investigated their stability in different gas environments. In oxidative gases like O_2, the Pt single atoms are stable at high temperatures (Fig. 2B). In the presence of reductive gases, either H_2 (Fig. 2C) or CO (Fig. 2D), however, facilitates the movement of the Pt atoms. It is observed that the strong interaction between CO and Pt weakens the binding of Pt to the support, or the dissociated H_2 molecules dislodge the surface oxygen-anchored Pt atoms, resulting in the formation of Pt clusters. Other reports have also indicated that reductive gases or functional groups can induce the movement of single metal atoms such as Pt[51,52] and Pd[53,54] in a CO atmosphere, leading to the destabilization of the single metal atoms. Similar to the destabilization effect of CO, adsorption of H_2 or H_2O can also induce sintering.[50,55] The H_2 or H_2O molecules are supposed to dissociatively adsorb on the metal atoms and then spill over to the metal–support interface to create –OH species. The produced –OH species further diffuse onto the oxide surface to consume lattice oxygen, resulting in the bond (M_1–O_n–) weakening.

However, the destabilization effect of reductive gases does not work universally for all metal–oxide SAC systems. Jakub *et al.*[44] have reported that, instead of accelerated sintering, CO adsorption can stabilize Ir adatoms to prevent their incorporation into the substrate. The formed IrCO species remains on the site until 610 K at which CO desorption takes place. In contrast, bare Ir single atoms incorporate into the substrate even below 100 K. CO adsorption makes the Ir atoms bond more strongly to the surface and the Ir–O bond length becomes shortened.

2.3 Surface free energy

Another approach to improve the stability of SACs is to mediate the surface free energy of the oxide support by the preparation of an ultrathin oxide film on a bulk metal substrate. In this method, the ultrathin oxide film is first grown on a metal single crystal surface. The electronic effect from the oxide–metal interface leads to a drastic surface property change of the grown thin oxide film, especially an increase in the surface free energy of the oxide film. Then the surface free energy or chemical potential of the supported single metal atoms becomes comparable to or even lower than that of the supported thin oxide film. As such, the single metal atoms are prevented from aggregating into nanoparticles. Distinguished from the strategy of the metal–oxide interaction, the SAC stability *via* the surface free energy approach is together regulated by the underlying oxide film and metal support. Zhou *et al.*[56] have successfully applied this methodology to prepare supported single-atom model catalysts, dispersed Au supported on an ultrathin CuO film grown on Cu(110) (Fig. 3A). The Au single atoms are stable upon warming up to 400 K, while thermal annealing at 500 K leads to a distinct decrease in the number of Au single atoms, leaving enlarged Au islands rather than particles at the surface. The Au atom can be precisely determined to be sitting at the

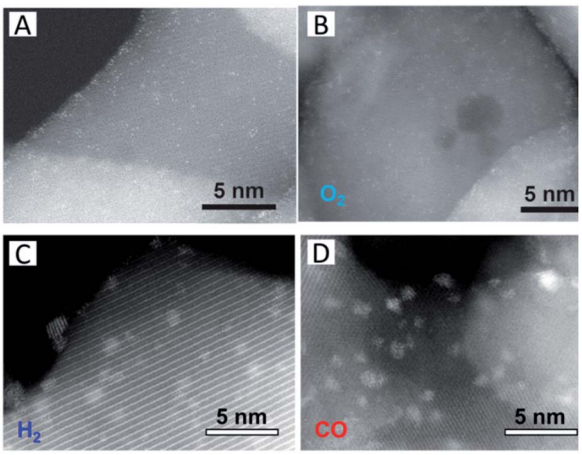

Fig. 2 (A) HAADF-STEM images of the as-prepared 1.66 wt% Pt_1/Fe_2O_3 SAC and the samples treated in (B) O_2, (C) H_2, and (D) CO at 250 °C for 2 h. Reproduced with permission.[50] Copyright 2018, IOP Publishing Ltd.

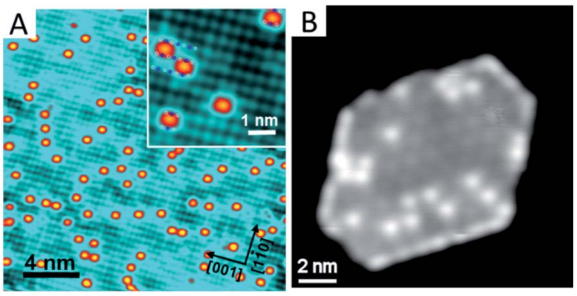

Fig. 3 (A) Au single atoms stabilized by monolayered CuO on a Cu(110) single crystal. Reproduced with permission.[56] Copyright 2018, American Chemical Society. (B) K single atoms stabilized by monolayered ceria on a Pt(111) single crystal. Reproduced with permission.[57] Copyright 2019, American Institute of Physics.

mid-point of two neighbouring O anions along the [1$\bar{1}$0] direction, and positioning inside the rectangle formed by four topmost neighbouring Cu cations. Chen *et al.*[57] have also obtained K single atoms with this method. They have employed a Pt(111) single crystal instead as the substrate to grow monolayered ceria islands, and then deposited K atoms on the ceria/Pt(111) sample (Fig. 3B). These K single atoms are stable above room temperature. Therrien *et al.*[58,59] have used a Cu_2O monolayer grown on the Cu(111) support to prepare Pt single atoms that are afterwards applied to catalyse CO oxidation and water activation. It can be seen that such a free energy approach to preparing single atoms is simple, straightforward and highly reproducible. In addition, the oxide film remains intact and the local ensemble environment of the metal atoms and their surrounding cations in the oxide is well defined, which is suitable to be characterized by scanning tunnelling microscopy at the atomic level.

3 Activity tunability

Numerous pieces of evidence have indicated that SACs normally show quite different catalytic performance compared to their nanoparticle counterparts. Such a difference has a tremendous impact on the activities of these entities, either a remarkable enhancement[46,60–63] or complete annihilation[12,64–66] for a specific catalytic process. Low coordination is also often regarded as a basic element for the high activity of SACs, although it is too simple to explain the various performances in reactions. As described in the Introduction section, charge and interface effects become more obvious for SACs than for their particle counterparts. Besides, it needs to be noted that not all single atoms perform well in given reactions. We hereby also present some cases in which nanoparticle catalysts catalytically outperform SACs.

3.1 Charge effect

Strong binding of a single metal atom to an oxide support usually leads to a charge transfer due to different electron affinities. The charge effect has been confirmed to be critical for catalytic performance in many cases, while the spectacular coordination environments of SACs on oxide supports can even generate a more sensitive charge effect than the metal particle catalysts do.

Recently Zhou *et al.*[56] have reported the vital role of the charge effect of Au adatoms in tuning their catalytic activity for CO oxidation. Au single atoms supported by a CuO monolayer are successfully prepared on a single crystalline Cu(110) substrate. The strong Au–O interaction gives rise to negatively charged Au atoms, as evidenced by X-ray photoemission spectroscopy. Once the Au_1/CuO sample is exposed to CO at room temperature (RT), O vacancies appear next to the Au single-atoms (Fig. 4A). These O vacancies are created by the reaction of CO with the O anions in the CuO lattice adjacent to the single Au atoms, which lead to neutralization of the negatively charged Au. The neutralized Au atoms turn out to be inactive for further CO oxidation (Fig. 4B). It is observed that the activity for CO oxidation is enhanced by the presence of negatively charged Au atoms through two possible ways. One is to weaken the Cu–O bond by electron withdrawal from the neighbouring oxygen atoms. The other is to activate the adsorbed CO molecules by enhancement of back-donation from the Au d-electrons to the anti-bonding π^* orbital of the adsorbed CO molecules.

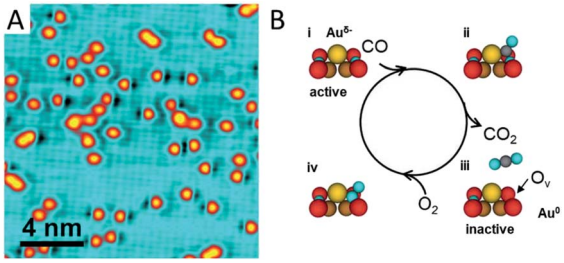

Fig. 4 CO oxidation catalysed by Au single atoms on the CuO monolayer. (A) STM image of the Au single atoms exposed to CO at RT. (B) Schematic illustration of the CO oxidation process activated by the Au single atoms on the CuO monolayer. Reproduced with permission.[56] Copyright 2018, American Chemical Society.

Fu *et al.*[67] have shown that doping the surface of TiO_2 with Pt single atoms enhances the formation of surface oxygen vacancies which are active redox centres for the selective cleavage of the C–O bonds *via* the reverse Mars–van Krevelen mechanism. They have revealed that the cationic redox Pt atoms on the TiO_2 surface are more active than metallic Pt particle sites for the C–O bond activation. Kwon *et al.*[62] have reported that Rh SACs can enable the conversion of methane to value-added products (methane or methanol) by using H_2O_2 or O_2 as oxidants below 300 °C, whereas Rh nanoparticles merely produce CO_2. The Rh single atoms dispersed on the ZrO_2 surface are oxidative in nature. It's also proven that the cationic Rh single atoms play a critical role in the stabilization of on-surface yielded CH_3 intermediates and prevention of their subsequent over-oxidation.

3.2 Interface effect

Since the interfaces between metal atoms and oxide supports are believed to be the location of the active sites in heterogeneous catalysis,[68] the interface effect may play a pivotal or even decisive role in shaping the catalytic performance of SACs. Lattice oxygen atoms at the interface in a metal/oxide system are conceived to be more reactive and selective than O_2 molecules in oxidation reactions.[69] Due to the metal–support interaction, single metal atoms frequently change the formation feasibility of O vacancies on oxide supports.

For example, Chen *et al.*[70] were able to prepare Pt/FeO_x catalysts with the Pt entity exclusively in single atom or nanoparticle states. The catalytic activity of the Pt/FeO_x catalyst has been experimentally identified to increase with the size decrease of the Pt entity. The supported Pt single atoms, however, turn out to be among the most active for the water–gas shift (WGS) reaction (Fig. 5A). Such high activity originates from the facilitation of the Pt adatoms to generate interfacial O vacancies on FeO_x. The produced O vacancies are able to

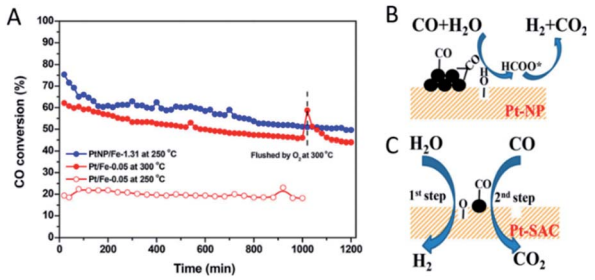

Fig. 5 (A) CO conversions as a function of time on stream during the WGS over Pt–SAC (Pt/Fe-0.05) at 250 and 300 °C, and Pt–NP (PtNP/Fe-1.31) at 250 °C, respectively. (B and C) Schematic illustration of the WGS activated by (B) Pt–NP and (C) Pt–SAC on FeO_x supports. Reproduced with permission.[70] Copyright 2018, American Chemical Society.

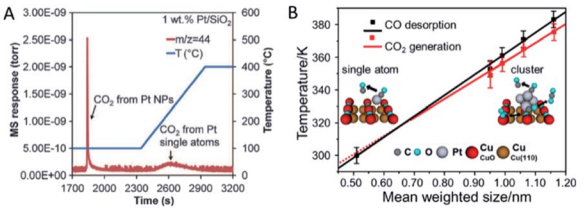

Fig. 6 (A) CO_2 signal monitored by the mass spectrum during the temperature-programmed oxidation process of the pre-adsorbed CO on Pt/SiO_2. Reproduced with permission.[73] Copyright 2015, American Association for the Advancement of Science. (B) Plots of the CO desorption and CO_2 generation temperatures *versus* the mean size of the Pt nanoclusters. Reproduced with permission.[13] Copyright 2016, American Chemical Society.

dissociate H_2O into H_2, and the lattice oxygen on the FeO_x surface can react with CO, which implies that a "redox" process takes place (Fig. 5C). In contrast, CO adsorbs more strongly on the Pt nanoparticles (Pt–NP) and subsequently reacts with the OH species generated by the activation of H_2O to form the formate intermediate, leading to a different pathway and lower activity for the WGS (Fig. 5B). Similar results are also observed in other SAC systems such as Rh/TiO_2 (ref. 60) and Pd/FeO_x,[71] where single metal atoms accelerate the formation of the O vacancies and show a higher activity towards the WGS than their counterparts, the metal nanoparticles, on the same catalytic support. Besides, SACs of the same active metal atoms sometimes exhibit varied catalytic activities upon dispersion on different oxides. For instance, the CO oxidation activity of Pt single atoms increases in sequence when the Pt adatoms are dispersed on γ-Al_2O_3, Fe_2O_3 and ZnO.[72] This interface effect between the catalytic activity and employed support can actually provide a novel strategy to regulate the SAC performance *via* support selection. The selectivity can be also enhanced by support selection through the oxide supporting effect.[20–22,49]

3.3 Counter examples

It should be noticed that SACs are not guaranteed to be more active than their nanoparticle counterparts. Many reported cases have indicated that some SACs have failed in certain catalytic reactions. Understanding the science behind the failure should help design high-performance SACs.

One reason is the varied adsorption capability of the reactants. Ding *et al.*[73] have demonstrated that only Pt nanoparticles show activity for CO oxidation and water–gas shift at low temperature in the coexistence of Pt single atoms and nanoparticles in many conventional catalysts. The lack of catalytic activity of Pt single atoms is partly attributed to their strong binding to the CO molecules (Fig. 6A). Zhou *et al.*[13] have reported another system of the Pt species on CuO films that the Pt nanoclusters have an optimized size for CO oxidation in the sub-nanometre regime, *i.e.* 0.7–1.1 nm. In contrast, Pt single atoms possess no reactivity for CO oxidation due to the early and complete desorption of CO before its oxidation on the model catalysts commences (Fig. 6B). Additionally, sub-nanometric Ir clusters have been reported to register a higher activity for CO oxidation than Ir single atoms with or without the presence of H_2.[14] This arises from the promotion effect of the Ir clusters on the CO adsorption and OH formation. On the one hand, sub-nanometric Ir clusters promote CO adsorption. On the other hand, H_2 can be feasibly activated and react with O species to form OH species. A subsequent reaction between the adsorbed CO and OH species possesses a lower activation energy, making the production of CO_2 rather feasible. On the contrary, Ir single atoms have a weaker CO adsorption capability and cannot activate the H_2 molecule so that the Ir single atoms exhibit a much lower activity for CO oxidation.

Another reason for the failure of SACs is the limitation of active sites. Complex reactions normally involve the activation, adsorption and migration of reactants and possible intermediates. SACs fail to provide continuously packed metal sites that can work cooperatively to complete these multiple steps. Zuo *et al.*[12] have reported that Ni single atoms are inactive for the complex dry reforming of the methane reaction, while Ni clusters show a higher performance for this reaction. This difference comes from the incapability of Ni single atoms to dissociate CO_2 and CH_4, while Ni clusters are able to activate both reactants and hence enable the production of CO, H_2, and H_2O.

4 Selectivity enhancement

4.1 Site limitation

Due to the lack of abundant metal sites, SACs have been reported to show poor performance for complex reactions and they may adopt a reaction mechanism completely different from that of their nanoparticle counterparts. This is often envisioned as a main drawback for SACs. However, such a disadvantage can be utilized to actually improve the selectivity of SACs under certain circumstances.

For instance, Millet *et al.*[49] have successfully prepared a Ni SAC by using a solid solution approach inside the MgO structure ($Ni_xMg_{1-x}O$). By controlling the reaction temperature, they are able to tune the formation of Ni clusters. Below 300 °C, the Ni SAC displays an astonishing selectivity for CO_2 hydrogenation towards CO production, avoiding over-reduction in the

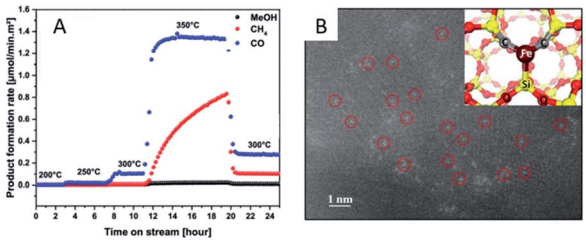

Fig. 7 (A) Product formation rate on the $Ni_xMg_{1-x}O$ samples at different temperatures. Reproduced with permission.[49] Copyright 2019, American Chemical Society. (B) STEM-HAADF image of the catalyst after the reaction, with the inset showing the computational model of the single iron atom bonded to two C atoms and one Si within the silica matrix. Reproduced with permission[15] Copyright 2014, American Association for the Advancement of Science.

reverse WGS reaction. An isolated Ni atom is capable of weakening the bond strength of CO_2 to a low-coordinated surface sites and promote H_2 dissociation. To obtain hydrogenation products such as CH_4 or MeOH, it is necessary to utilize the Ni clusters that are formed above 300 °C (Fig. 7A). Guo *et al.*[15] have demonstrated an atom-economical direct CH_4 conversion process, enabled by lattice-confined single iron sites embedded within a silica matrix, which can activate CH_4 and generate methyl radicals. The absence of adjacent iron sites prevents catalytic C–C coupling, further oligomerization, and hence coke deposition (Fig. 7B). Xie *et al.*[74] have reported that Pt_1/CeO_2 catalysts exhibit a catalytic performance superior to their nanoparticle counterparts, achieving 14.4% of methane conversion at 975 °C and 74.6% selectivity toward C_2 products (ethane, ethylene, and acetylene). Comparative studies of Pt_1/CeO_2 catalysts of different loadings and the nanoparticle counterparts have revealed that Pt single atoms are the active sites for the selective conversion of methane into C_2 hydrocarbons.

5 Summary and perspectives

This minireview overviews some recent advancements in exploring the intrinsic principles of oxide-supported SACs in catalytic performance, including stability, activity and selectivity. A consensus has been reached that some SACs possess distinctive and even unique properties against their nanoparticle counterparts. Such a difference in catalytic performance could not be linearly scaled by the simple size effect. SACs have their own merits in heterogeneous catalysis, including remarkable enhancement or complete annihilation for catalytic activity, simplification of reaction pathways, generation of new products, and cost-effective preparation of catalysts containing precious metals. Therefore, SACs do provide a new opportunity for catalyst design and development. The catalytic performance of SACs is largely determined by governing principles including metal–oxide interaction, surface free energy, charge effect, interface effect, site limitation and so on. These intrinsic properties may be traded off to improve the catalytic performance of SACs. Comprehensive consideration is required to develop a practical catalyst that meets the main criteria: high stability, excellent catalytic activity and high selectivity toward target products.

In the foreseeable future, more and more SACs with unique properties are anticipated to appear due to the remarkable advancements in nanoscience and technology. Until today, most SACs have been exploited for relatively simple catalytic reactions. Multi-electron complex catalytic reactions have already appeared on the new horizon because more and more bi-metallically alloyed SACs have been reported in the literature that are beyond the scope of this minireview.[29] At the present stage, more SACs should be tried and tested to build up a practical database that may be analysed with artificial intelligence to uncover the unknown principles of heterogeneous catalytic processes. In addition, it should be pointed out that heterogeneous catalysts undergo rigorous dynamic changes in both chemical states and structures under reaction conditions that instantly vary the reaction mechanisms in their ever-changing reaction atmospheres. The majority of our present knowledge about heterogeneous catalysis is built upon "static" catalytic models and pictures. This can lead to contradictory and frustrating conclusions.[75] To tackle these challenging issues, detailed and systematic observations, characterization studies and analyses at the atomic level are highly needed to establish the exact connections between various structures of reactants and catalysts with specific catalytic characteristics.[76,77] Such an atomic-level understanding will provide valuable guidance in designing and preparing advanced catalysts.[24,78–86] Moreover, *in situ* and *operando* studies concerning the dynamic changes during the catalytic reactions are required to further reveal the mechanism involved in catalysis. Compared with SACs made by wet chemistry that are indeed closer to practical applications, single atoms fabricated by physical deposition on ultrathin oxide films (surface free energy approach) provide better-defined models for fundamental studies, especially for local and dynamic characterization studies, of practical catalysts.

Conflicts of interest

There are no conflicts to declare.

Acknowledgements

This work was jointly supported by the NSFC (21821004 and 21932001) and MOST (2017YFA0204702), China.

References

1 X. Zhang, Z. Sun, B. Wang, Y. Tang, N. Luan, Y. Li and F. F. Tao, *J. Am. Chem. Soc.*, 2018, **140**, 954–962.
2 Z. Chen, V. Evgeniya, M. Sharon, F. Edvin, M. A. Ortuño, L. Núria, S. M. Collins, P. A. Midgley, R. Sylvia, V. Gianvito and J. Pérez-Ramírez, *Nat. Nanotechnol.*, 2018, **13**, 702–707.
3 Y. Peng, Z. Geng, S. Zhao, L. Wang, H. Li, X. Wang, X. Zheng, J. Zhu, Z. Li, R. Si and J. Zeng, *Nano Lett.*, 2018, **18**, 3785–3791.

4 E. Vorobyeva, E. Fako, Z. Chen, S. M. Collins, D. Johnstone, P. A. Midgley, R. Hauert, O. V. Safonova, G. Vilé and N. López, *Angew. Chem., Int. Ed.*, 2019, **58**, 8724–8729.
5 R. Lin, D. Albani, E. Fako, S. K. Kaiser, O. V. Safonova, N. López and J. Pérez-Ramírez, *Angew. Chem., Int. Ed.*, 2018, **58**, 514–519.
6 S. Wei, A. Li, J. C. Liu, L. Zhi, W. Chen, G. Yue, Q. Zhang, C. Weng-Chon, W. Yu, L. Zheng, H. Xiao, C. Chen, D. Wang, Q. Peng, L. Gu, X. Han, J. Li and Y. Li, *Nat. Nanotechnol.*, 2018, **13**, 856–861.
7 B. Qiao, A. Wang, X. Yang, L. F. Allard, Z. Jiang, Y. Cui, J. Liu, J. Li and T. Zhang, *Nat. Chem.*, 2011, **3**, 634–641.
8 A. Sanchez, S. Abbet, U. Heiz, W.-D. Schneider, H. Hakkinen, R. N. Barnett and U. Landman, *J. Phys. Chem. A*, 1999, **103**, 9573–9578.
9 M. J. Berr, F. F. Schweinberger, M. Döblinger, K. E. Sanwald, C. Wolff, J. Breimeier, A. S. Crampton, C. J. Ridge, M. Tschurl, U. Heiz, F. Jackel and F. Jochen, *Nano Lett.*, 2012, **12**, 5903–5906.
10 J. N. Kuhn, W. Huang, C.-K. Tsung, Y. Zhang and G. A. Somorjai, *J. Am. Chem. Soc.*, 2008, **130**, 14026–14027.
11 J. Wang, H. Tan, S. Yu and K. Zhou, *ACS Catal.*, 2015, **5**, 2873–2881.
12 Z. Zuo, S. Liu, Z. Wang, C. Liu, W. Huang, J. Huang and P. Liu, *ACS Catal.*, 2018, **8**, 9821–9835.
13 X. Zhou, W. Yang, Q. Chen, Z. Geng, X. Shao, J. Li, Y. Wang, D. Dai, W. Chen, G. Xu, X. Yang and K. Wu, *J. Phys. Chem. C*, 2016, **120**, 1709–1715.
14 J. Lin, Y. Chen, Y. Zhou, L. Li, B. Qiao, A. Wang, J. Liu, X. Wang and T. Zhang, *AIChE J.*, 2017, **63**, 4003–4012.
15 X. Guo, G. Fang, G. Li, H. Ma, H. Fan, L. Yu, C. Ma, X. Wu, D. Deng, M. Wei, D. Tan, R. Si, S. Zhang, J. Li, L. Sun, Z. Tang, X. Pan and X. Bao, *Science*, 2014, **344**, 616–619.
16 B. B. Sarma, J. Kim, J. Amsler, G. Agostini, C. Weidenthaler, N. Pfander, R. Arenal, P. Concepcion, P. N. Plessow, F. Studt and G. Prieto, *Angew. Chem.*, 2020, **132**, 5806–5815.
17 Y. Wang, H. Arandiyan, J. Scott, K.-F. Aguey-Zinsou and R. Amal, *ACS Appl. Energy Mater.*, 2018, **1**, 6781–6789.
18 S. Zhao, Y. Wen, X. Liu, X. Pen, F. Lü, F. Gao, X. Xie, C. Du, H. Yi, D. Kang and X. Tang, *Nano Res.*, 2020, **13**, 1544–1551.
19 M. Babucci, C. Fang, J. E. Perezaguilar, A. S. Hoffman, A. Boubnov, E. Guan, S. R. Bare, B. C. Gates and A. Uzun, *Chem. Sci.*, 2019, **10**, 2623–2632.
20 E. Guan, L. M. Debefve, M. Vasiliu, S. Zhang, D. A. Dixon and B. C. Gates, *ACS Catal.*, 2019, **9**, 9545–9553.
21 S. Tada, T. Shimizu, H. Kameyama, T. Haneda and R. Kikuchi, *Int. J. Hydrogen Energy*, 2012, **37**, 5527–5531.
22 Y. Chen, Z. Huang, M. Zhou, Z. Ma, J. Chen and X. Tang, *Environ. Sci. Technol.*, 2017, **51**, 2304–2311.
23 S. Li, Y. Xu, Y. Chen, W. Li, L. Lin, M. Li, Y. Deng, X. Wang, B. Ge, C. Yang, S. Yao, J. Xie, Y. Li, X. Liu and M. Ding, *Angew. Chem.*, 2017, **56**, 10761–10765.
24 Z. Huang, Z. Xu, J. Zhou, H. Chen, W. Rong, Y. Lin, X. Wen, H. Zhu and K. Wu, *J. Phys. Chem. C*, 2019, **123**, 17823–17828.
25 A. Wang, J. Li and T. Zhang, *Nat. Rev. Chem.*, 2018, **2**, 65–81.
26 H. Schwarz, *Catal. Sci. Technol.*, 2017, **7**, 4302–4314.
27 C. Zhu, S. Fu, Q. Shi, D. Du and Y. Lin, *Angew. Chem., Int. Ed.*, 2017, **56**, 13944–13960.
28 H. Zhang, G. Liu, L. Shi and J. Ye, *Adv. Energy Mater.*, 2018, **8**, 1701343.
29 G. Giannakakis, M. Flytzani-Stephanopoulos and E. C. H. Sykes, *Acc. Chem. Res.*, 2019, **52**, 237–247.
30 M. T. Darby, M. Stamatakis, A. Michaelides and E. C. H. Sykes, *J. Phys. Chem. Lett.*, 2018, **9**, 5636–5646.
31 X. Cui, W. Li, P. Ryabchuk, K. Junge and M. Beller, *Nat. Catal.*, 2018, **1**, 385–397.
32 S. Liang, C. Hao and Y. Shi, *ChemCatChem*, 2015, **7**, 2559–2567.
33 X.-F. Yang, A. Wang, B. Qiao, J. Li, J. Liu and T. Zhang, *Acc. Chem. Res.*, 2013, **46**, 1740–1748.
34 J. Liu, *ACS Catal.*, 2017, **7**, 34–59.
35 J. Liu, *Chin. J. Catal.*, 2017, **38**, 1460–1472.
36 Z. Li, D. Wang, Y. Wu and Y. Li, *Natl. Sci. Rev.*, 2018, **5**, 673–689.
37 Y. Chen, S. Ji, C. Chen, Q. Peng, D. Wang and Y. Li, *Joule*, 2018, **2**, 1242–1264.
38 M. J. Hülsey, J. Zhang and N. Yan, *Adv. Mater.*, 2018, **30**, 1802304.
39 L. Liu and A. Corma, *Chem. Rev.*, 2018, **118**, 4981–5079.
40 Y. Wang, J. Mao, X. Meng, L. Yu, D. Deng and X. Bao, *Chem. Rev.*, 2019, **119**, 1806–1854.
41 Y. Guo, R. Lang and B. Qiao, *Catalysts*, 2019, **9**, 135.
42 G. S. Parkinson, *Catal. Lett.*, 2019, **149**, 1137–1146.
43 Z. W. Chen, L. X. Chen, C. C. Yang and Q. Jiang, *J. Mater. Chem. A*, 2019, **7**, 3492–3515.
44 Z. Jakub, J. Hulva, M. Meier, R. Bliem, F. Kraushofer, M. Setvin, M. Schmid, U. Diebold, C. Franchini and G. S. Parkinson, *Angew. Chem., Int. Ed.*, 2019, **58**, 13961–13968.
45 M. Meier, Z. Jakub, J. Balajka, J. Hulva, R. Bliem, P. K. Thakur, T.-L. Lee, C. Franchini, M. Schmid, U. Diebold, F. Allegretti, D. A. Duncan and G. S. Parkinson, *Nanoscale*, 2018, **10**, 2226–2230.
46 Z. Zhang, Y. Zhu, H. Asakura, B. Zhang, J. Zhang, M. Zhou, Y. Han, T. Tanaka, A. Wang, T. Zhang and N. Yan, *Nat. Commun.*, 2017, **8**, 16100.
47 H. V. Thang, G. Pacchioni, L. DeRita and P. Christopher, *J. Catal.*, 2018, **367**, 104–114.
48 H. V. Thang, S. Tosoni, L. Fang, P. Bruijnincx and G. Pacchioni, *ChemCatChem*, 2018, **10**, 2634–2645.
49 M.-M. Millet, G. Algara-Siller, S. Wrabetz, A. Mazheika, F. Girgsdies, D. Teschner, F. Seitz, A. Tarasov, S. V. Levchenko, R. Schlögl and E. Frei, *J. Am. Chem. Soc.*, 2019, **141**, 2451–2461.
50 S. Duan, R. Wang and J. Liu, *Nanotechnology*, 2018, **29**, 204002.
51 R. Bliem, J. E. V. D. Hoeven Je, J. Hulva, J. Pavelec, O. Gamba, P. E. de Jongh, M. Schmid, P. Blaha, U. Diebold and G. S. Parkinson, *Proc. Natl. Acad. Sci. U. S. A.*, 2016, **113**, 8921–8926.
52 L. DeRita, J. Resasco, S. Dai, A. Boubnov, H. V. Thang, A. S. Hoffman, I. Ro, G. W. Graham, S. R. Bare,

G. Pacchioni, X. Pan and P. Christopher, *Nat. Mater.*, 2019, **18**, 746–751.
53 G. S. Parkinson, Z. Novotny, G. Argentero, M. Schmid, J. Pavelec, R. Kosak, P. Blaha and U. Diebold, *Nat. Mater.*, 2013, **12**, 724–728.
54 G. Spezzati, Y. Su, J. P. Hofmann, A. D. Benavidez, A. T. DeLaRiva, J. McCabe, A. K. Datye and E. J. M. Hensen, *ACS Catal.*, 2017, **7**, 6887–6891.
55 D. B. Rasmussen, T. V. W. Janssens, B. Temel, T. Bligaard, B. Hinnemann, S. Helveg and J. Sehested, *J. Catal.*, 2012, **293**, 205–214.
56 X. Zhou, Q. Shen, K. Yuan, W. Yang, Q. Chen, Z. Geng, J. Zhang, X. Shao, W. Chen, G. Xu, X. Yang and K. Wu, *J. Am. Chem. Soc.*, 2018, **140**, 554–557.
57 H. Chen, W. Rong, Z. Huang, Z. Peng, Z. Xu, J. Zhou, B. Di, X. Zhou and K. Wu, *J. Chem. Phys.*, 2019, **151**, 184703.
58 A. J. Therrien, A. J. R. Hensley, M. D. Marcinkowski, R. Zhang, F. R. Lucci, B. Coughlin, A. C. Schilling, J. S. McEwen and E. C. H. Sykes, *Nat. Catal.*, 2018, **1**, 192–198.
59 A. J. Therrien, G. Kyle, A. J. R. Hensley, A. C. Schilling, R. T. Hannagan, M. D. Marcinkowski, P. Alex, F. R. Lucci, E. C. H. Sykes and M. E. Jean-Sabin, *J. Catal.*, 2018, **364**, 166–173.
60 H. Guan, J. Lin, B. Qiao, S. Miao, A.-Q. Wang, X. Wang and T. Zhang, *AIChE J.*, 2017, **63**, 2081–2088.
61 C. Yang, L. Jian, L. Lin, B. Qiao, J. Liu, Y. Su and X. Wang, *ACS Catal.*, 2018, **8**, 859–868.
62 Y. Kwon, T. Y. Kim, G. Kwon, J. Yi and H. Lee, *J. Am. Chem. Soc.*, 2017, **139**, 17694–17699.
63 J. Shan, M. Li, L. F. Allard, S. Lee and M. Flytzani-Stephanopoulos, *Nature*, 2017, **551**, 605–608.
64 S. Zhang, Y. Tang, L. Nguyen, Y. F. Zhao, Z. Wu, T. W. Goh, J. J. Liu, Y. Li, T. Zhu, W. Huang, A. I. Frenkel, J. Li and F. F. Tao, *ACS Catal.*, 2018, **8**, 110–121.
65 C. Dessal, L. Martínez, C. Maheu, T. Len, F. Morfin, J. L. Rousset, E. Puzenat, P. Afanasiev, M. Aouine, L. Soler, J. Llorca and L. Piccolo, *J. Catal.*, 2019, **375**, 155–163.
66 C. K. Narula, L. F. Allard, M. Moses-Debusk, G. M. Stocks and Z. Wu, *Sci. Rep.*, 2017, **7**, 560.
67 J. Fu, J. Lym, W. Zheng, K. Alexopoulos, A. V. Mironenko, N. Li, J. A. Boscoboinik, D. Su, R. T. Weber and D. G. Vlachos, *Nat. Catal.*, 2020, **3**, 446–453.
68 G. Zhao, Y. Fan, Z. Chen, Q. Liu, Y. Ji, Z. Yi, Z. Niu, J. Mao, X. Bao and P. Hu, *Nat. Commun.*, 2017, **8**, 14039.
69 T. Li, F. Liu, Y. Tang, L. Li, S. Miao, Y. Su, J. Zhang, J. Huang, H. Sun, M. Haruta, A. Wang, B. Qiao, J. Li and T. Zhang, *Angew. Chem., Int. Ed.*, 2018, **57**, 7795–7799.
70 Y. Chen, J. Lin, L. Li, B. Qiao, J. Liu, Y. Su and X. Wang, *ACS Catal.*, 2018, **8**, 859–868.
71 X. Sun, J. Lin, Y. Zhou, L. Lin, Y. Su, X. Wang and T. Zhang, *AIChE J.*, 2017, **63**, 4022–4031.
72 Y. Lou and J. Liu, *Ind. Eng. Chem. Res.*, 2017, **56**, 6916–6925.
73 K. Ding, A. Gulec, A. M. Johnson, N. M. Schweitzer, G. D. Stucky, L. D. Marks and P. C. Stair, *Science*, 2015, **350**, 189–192.
74 P. Xie, T. Pu, A. Nie, S. Hwang, S. C. Purdy, W. Yu, D. Su, J. T. Miller and C. Wang, *ACS Catal.*, 2018, **8**, 4044–4048.
75 S. C. Ammal and A. Heyden, *ACS Catal.*, 2017, **7**, 301–309.
76 H. Chen, H. Zhu, Z. Huang, W. Rong and K. Wu, *Adv. Mater.*, 2019, **31**, 1902080.
77 L. Xing, Z. Peng, W. Li and K. Wu, *Acc. Chem. Res.*, 2019, **52**, 1048–1058.
78 F. Dvořak, M. F. Camellone, A. Tovt, N. Tran, F. R. Negreiros, M. Vorokhta, T. Skala, I. Matolinova, J. Myslivecek, V. Matolin and S. Fabris, *Nat. Commun.*, 2016, **7**, 10801.
79 B. Zhang, H. Asakura, J. Zhang, J. Zhang, S. De and N. Yan, *Angew. Chem.*, 2016, **55**, 8319–8323.
80 J. Ftouni, A. Muñoz-Murillo, A. Goryachev, J. P. Hofmann, E. J. M. Hensen, L. Lu, C. J. Kiely, P. C. A. Bruijnincx and B. M. Weckhuysen, *ACS Catal.*, 2016, **6**, 5462–5472.
81 L. Liu, U. Diaz, R. Arenal, G. Agostini, P. Concepcion and A. Corma, *Nat. Mater.*, 2017, **16**, 132–138.
82 H. Fei, J. Dong, M. J. Arellanojimenez, G. Ye, N. D. Kim, E. L. G. Samuel, Z. Peng, Z. Zhu, F. Qin, J. Bao, M. J. Yacaman, P. M. Ajayan, D. Chen and J. M. Tour, *Nat. Commun.*, 2015, **6**, 8668.
83 J. Fu, J. Lym, W. Zheng, K. Alexopoulos, A. V. Mironenko, N. Li, J. A. Boscoboinik, D. Su, R. T. Weber and D. G. Vlachos, *Nat. Catal.*, 2020, **3**, 446–453.
84 C. Kuo, Y. Lu, L. Kovarik, M. H. Engelhard and A. M. Karim, *ACS Catal.*, 2019, **9**, 11030–11041.
85 Z. Lu, X. Liu, B. Zhang, Z. Gan, S. Tang, L. Ma, T. Wu, G. J. Nelson, Y. Qin, C. H. Turner and Yu Lei, *J. Catal.*, 2019, **377**, 419–428.
86 A. Aitbekova, L. Wu, C. J. Wrasman, A. Boubnov, A. S. Hoffman, E. D. Goodman, S. R. Bare and M. Cargnello, *J. Am. Chem. Soc.*, 2018, **140**, 13736–13745.
87 J. Kim, C. W. Roh, S. K. Sahoo, S. Yang, J. Bae, J. W. Han and H. Lee, *Adv. Energy Mater.*, 2018, **8**, 1701476.